

Effect of aromaticity on soot formation: A reactive molecular dynamics study

Deniz Kaya Eyice*, Kevin Wan[†], Julien Manin[‡]
Sandia National Laboratories, Livermore, CA, 94550, USA

Francisco J. Guzman[§]
NASA Glenn Research Center, Cleveland, Ohio, 44135, USA

This study investigates the formation of soot from n-dodecane and its blend with m-xylene under pyrolytic and low-oxygen conditions with reactive molecular dynamics (MD) simulations. ReaxFF force field is used to simulate the interactions of fuel and oxygen molecules at engine-relevant conditions (2500-3500 K and 70-75 bar). Fuel molecules with carbon atom density of 0.03 g/cm³ are dispersed into a cube and constant temperature simulations are carried out with a Nosé-Hoover thermostat. Pyrolysis of n-dodecane and the chemical pathway towards the formation of aromatic hydrocarbons are investigated. The initial pyrolysis rate of n-dodecane is observed to be slightly higher with the addition of aromatic compounds and oxygen. While the first aromatics formed from the decomposed n-dodecane are phenyl radicals at 2500 K, decomposition of the aliphatic fuel compound is observed to be necessary to build a carbon cluster, and eventually soot. Morphological properties of the created soot particles are also analyzed. The maturity, size and aromatics content of the soot particle are slightly affected with the addition of m-xylene and oxygen at 3500 K within the 3 ns simulation time possibly due the formation of larger and more condensed aromatic rings, resulting in larger soot molecules. The outcomes of this study provide important insights into the formation mechanism of soot and its morphological characteristics depending on varying fuel concentrations at pyrolysis and low-oxygen engine conditions. Results of this analysis will further contribute to the understanding of contrail formation on generated soot particles originated from the combustion of different chemical components with particle chemistry matching companion experiments.

I. Nomenclature

MD	=	Molecular Dynamics
NVT	=	Number, Volume, Temperature
PAH	=	Polycyclic Aromatic Hydrocarbon
QM	=	Quantum Methods
SAF	=	Sustainable Aviation Fuel

II. Introduction

Recent studies indicate that the impact of contrail formation on climate change is significant, with scientific evidence highlighting the role of soot particles in this process. However, the relationship between soot particles and contrail formation is not yet fully understood and requires detailed investigation to effectively decarbonize aviation [1, 2]. Addressing this issue is crucial, as aircraft-induced clouds contribute to radiative forcing [3] and have an equal or greater impact on climate change compared to CO₂ emissions [2]. While sustainable aviation fuels (SAFs) become a valuable alternative to petroleum-based fuels for lowering the environmental impacts on aviation, it is crucial to investigate the formation of soot and contrails from SAF fuel components and to fine-tune these fuels to effectively reduce their sooting propensities and prevent soot emissions [4].

*Postdoctoral Researcher, Combustion Research Facility, Applied Combustion Research I.

[†]Postdoctoral Researcher, Combustion Research Facility, Applied Combustion Research I.

[‡]Principal Member of the Technical Staff, Combustion Research Facility, Applied Combustion Research I.

[§]Research Chemical Engineer, Engine Combustion Branch, AIAA Senior Member.

The influence of polycyclic aromatic hydrocarbons (PAHs) on soot growth is widely accepted, however, there remains considerable debate regarding their precise role as precursors. The mechanism of soot formation is complex and influenced by various factors including the chemical composition of the fuel, temperature, pressure, oxygen concentration and residence time etc. The formation of soot from different hydrocarbons has been extensively studied, revealing significant insights into the contributions of various chemical groups under both pyrolytic and oxidative conditions [5, 6]. Pyrolytic conditions are often preferred to investigate the chemical pathways in soot formation from surrogate components without the complicating effects of oxidation [7–10]. Zeng et al. studied the pyrolysis of n-dodecane under various pressures and temperatures using a flow reactor exploring the influence of carbon chain length on the pyrolysis reactivity, ignition delay times, and laminar burning velocities of n-alkanes on the developed kinetic model [11]. They observed the formation of benzene initiated from C3 species as a soot precursor. Kashiwa et al. studied the effect of PAHs and oxygen addition on the soot formation mechanism from benzene pyrolysis [12]. According to their experimental data, the concentration of naphthalene created from benzene pyrolysis with oxygen was higher than the concentration of biphenyl formed from benzene pyrolysis without oxygen. Similarly, Busillo et al. reported that while the low temperature and oxygen concentration increases the soot yield of acetylene, the presence of oxygen also changes the chemical pathway towards the PAH formation [13]. Herbinet et al. studied thermal decomposition of n-dodecane at 773-1073 K in a jet stirred reactor and they pointed out that benzene and its related radicals including cyclopentadienyl, phenyl and benzyl radicals, contributes significantly to the development of heavier aromatics and poly-aromatic species [14].

While the formation of radicals and soot precursors can be measured experimentally under various conditions, atomistic simulations can provide extensive information on the chemical pathway, kinetics and the characteristics of soot particles. Quantum methods (QM), offer a profound understanding of the intricate chemistry underlying soot formation [15]. However, the computational demands of such approaches are considerable, often limiting their applicability to smaller systems or short time scales. As an alternative, molecular dynamics (MD) simulations coupled with reactive force fields emerge as a pragmatic solution, providing valuable insights into soot formation processes at a reduced computational cost [16, 17]. These simulations fill the gap between experimental observations and theoretical models, allowing the development of more accurate and predictive models of soot formation and particle characterization. Many MD studies report possible pathways and intermediate molecules during the pyrolysis of fuel molecules. Zhang et al. studied the formation of soot from acetylene molecules at 1500 K with ReaxFF and they concluded that polyynes and polyenes are typically present in the products of acetylene pyrolysis [18]. Wang et al. proposed two pathways on the pyrolysis of dodecane at 2000-3000 K: (1) the cleavage of C–C bond to form smaller hydrocarbon radicals and the dehydrogenation reaction to form an H radical and the corresponding n-C₁₂H₂₅ radical, (2) H abstraction reactions by small radicals including H, CH₃, and C₂H₅ [19].

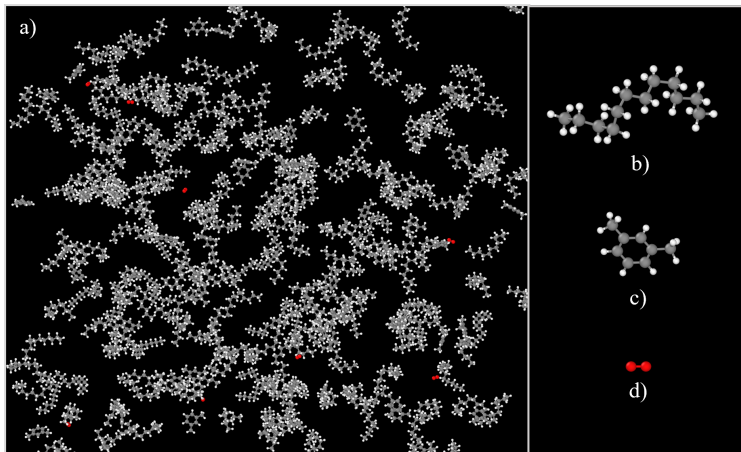
In this study, the formation mechanism of soot from aliphatic fuel surrogate, n-dodecane is studied via reactive MD simulations at aero-engine conditions. Simulations are carried out with LAMMPS at constant temperature with the ReaxFF force field which is developed to capture hydrocarbon pyrolysis and carbon condensation. Effect of initial aromatic content of the fuel mixture is investigated at pyrolysis and oxygenated conditions. Chemical pathways toward the formation of aromatic rings and soot clusters and the morphological properties of the formed soot particles are analyzed.

III. Molecular Dynamics Simulations

ReaxFF simulations are performed using different hydrocarbon mixtures: pure n-dodecane (C₁₂H₂₆), a mixture of n-dodecane and m-xylene (C₈H₁₀) in an 80:20 ratio, and a mixture of n-dodecane, m-xylene at the same ratio with 3% oxygen (O₂). The number of molecules and the volume fractions of the species are reported in Table 1. Each simulation maintains a carbon atom density of 0.03 g/cm³ within a 118x118x118 Å³ box with periodic boundary conditions, corresponding to a pressure of approximately 75 bar. To eliminate the influence of initial configuration on the simulation results, each ReaxFF simulation is repeated three times with a random molecular distribution within the domain generated using Packmol [20]. Constant temperature simulations are conducted at aero-engine flame temperatures, 2500 K and elevated temperatures, 3500 K to investigate the chemical pathway towards the aromatic cluster formation and the morphology of the soot particles, respectively. Fig. 1 reports the initial molecule configuration of the simulation including n-dodecane, m-xylene and oxygen molecules.

Table 1 Molecular composition of the fuel blends.

	Number of molecules			Volume fraction of molecules		
	n-dodecane	m-xylene	oxygen	n-dodecane	m-xylene	oxygen
<i>n-dodecane</i>	200	-	-	1.0	0	0
<i>n-dodecane + m-xylene</i>	200	50	-	0.80	0.20	0
<i>n-dodecane + m-xylene + O₂</i>	200	50	8	0.78	0.19	0.03

**Fig. 1 (a) Initial configuration of the simulation setup b) n-dodecane molecule c) m-xylene molecule and d) oxygen molecule. C, H and O atoms are represented in gray, white and red, respectively.**

The equations of motion are integrated with a time step of 0.1 fs using the velocity Verlet algorithm at constant number, volume, and temperature (NVT) conditions and temperature is controlled using Nosé-Hoover thermostat with a damping constant of 100 fs. The system was first equilibrated at 300 K for 10 ps. The temperature was then increased to the production run temperature over 10 ps. All ReaxFF molecular dynamics simulations are performed using an open-source molecular dynamics simulator, LAMMPS [21, 22] with ReaxFF [16] for 3 ns. The reactive force field by Ashraf and van Duin is used to simulate the chemical reactivity under pyrolysis conditions since it is reported to produce improved C1 chemistry predictions from atomistic level, as well as the detailed chemistry of oxidation and pyrolysis of long-chain hydrocarbons and carbon condensation [23]. Chemical reaction pathway analysis is performed using ChemTraYzer algorithm [24]. In order to analyze the molecular structures in terms of aromaticity, MAFIAMD is utilized [25]. All computations are performed on the Sandia National Laboratories supercomputers using 64 Intel(R) Xeon(R) Gold 6226R CPUs.

IV. Results

As described previously, ReaxFF simulations were performed with n-dodecane, n-dodecane + m-xylene (80:20) mixture and dodecane + m-xylene (80:20) mixture with 3% oxygen. Kinetic interpretations and chemical pathway analyses are conducted using low temperature simulations, 2500 K due to their better resemblance of real-life conditions in engines. Since the high temperatures lead to soot formation in a shorter timescale, high temperature simulations at 3500 K are utilized to analyze the soot structure.

In Fig. 2, pyrolysis of n-dodecane molecules at 2500 K is reported. Solid lines indicate the average of three repetition simulations for each initial configuration of molecules while the area around them shows the minimum and maximum values for each individual simulation. In order to make a better comparison of the species, all molecules reported in this manuscript are normalized by the initial amount of n-dodecane molecules. At the beginning, each case has 200 n-dodecane molecules and it is observed that all of them are decomposed within 0.20 ns. The consistency of the molecular decomposition of the fuel molecules with and without oxygen indicates that at such concentration

level, oxygen only bears minimal effect. This is likely the result of the relatively high ambient temperature, which better supports thermal decomposition over oxygen-induced oxidation. The early stages of n-dodecane decomposition is not affected by the initial configuration of the molecules. However, as the smaller molecules are formed, the rate of decomposition is slightly affected, especially in the presence of other compounds, i.e. m-xylene and oxygen, since they can facilitate side reactions. The maximum variation is computed as 5.3% for n-dodecane + m-xylene + O₂ case and it is assumed that the initial randomness of the molecules does not have a significant impact on the results at the performed conditions. Therefore, for the sake of clarity, average values of the repetition simulations are reported in the following sections of the manuscript.

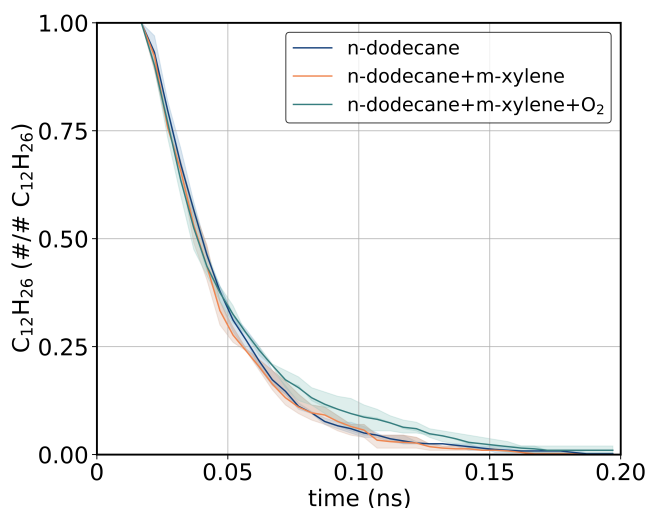


Fig. 2 Consumption of n-dodecane molecules within time at 2500 K. The amount of molecules are normalized by the initial amount of fuel molecules. Solid lines represent the average of the repetition simulations for each case and area around these line represents the minimum and maximum values from each repetition simulations.

In order to have a deeper analysis, the change in the time derivative of the normalized n-dodecane consumption in time is reported in Fig. 3. The presence of 20% aromatic compounds facilitates the decay rate of n-dodecane molecules at initial stages, likely due to additional pathways enabled by the aromatic compound. In the meantime, the decomposition of n-dodecane molecules are slightly delayed in the presence of oxygen molecules. This is possibly due to the oxygenation of intermediates and radicals, forming new species that may inhibit or slow down the overall consumption of n-dodecane. However, the overall rate of n-dodecane pyrolysis is not affected significantly by the initial molecule configuration at the performed conditions. Instead, the presence of oxygen and m-xylene facilitates chemical pathways that give rise to these differences.

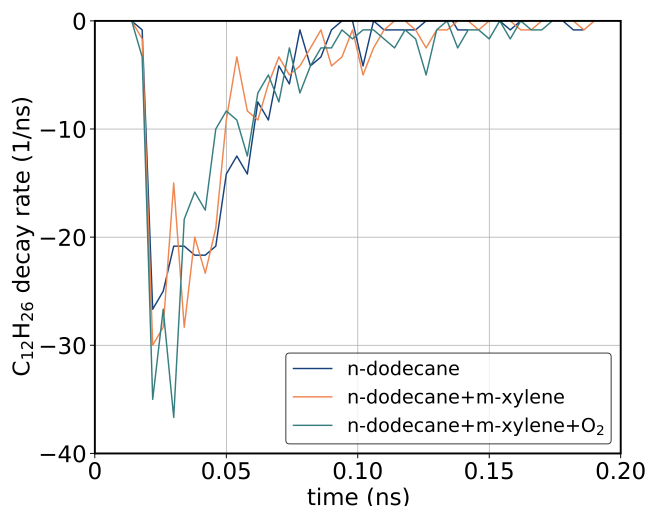


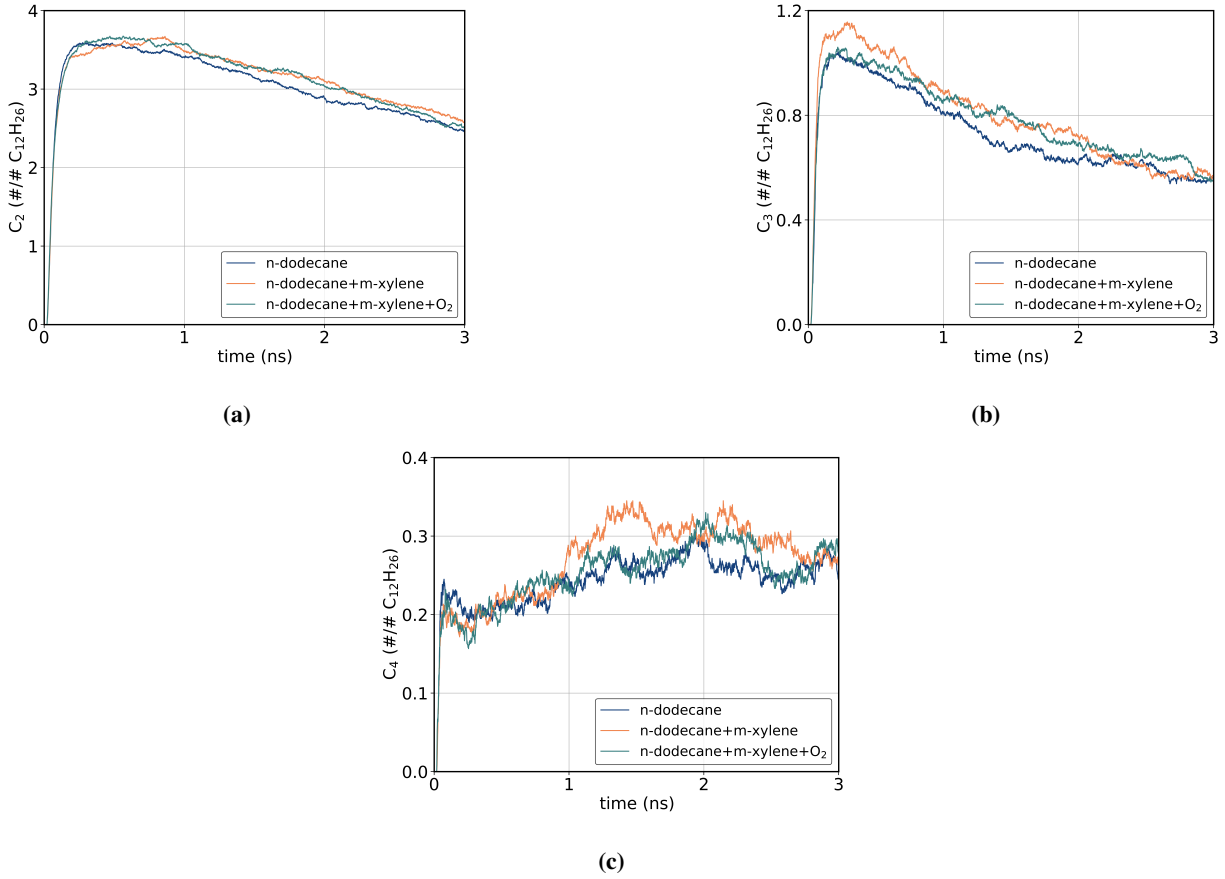
Fig. 3 Decay rate of n-dodecane molecules within time at 2500 K.

Pyrolysis reactions of n-dodecane are investigated and the initial decomposition reactions of n-dodecane and their probabilities are reported in Table 2. Only low temperature simulation results are given due to the fact that in higher temperature simulations, at 3500 K, the pyrolysis reactions are happening within a very short time making the system harder to analyze at the current resolution of reaction steps. Moreover, complex aromatics are forming during the intermediate steps towards soot formation and the analysis of these intermediates is neither computationally feasible nor accurate. Temperatures around 2500 K are close to realistic conditions at aero-engines to study the reaction pathway. Most of the studies, however, have been investigated dodecane pyrolysis at temperatures ranging from 770 to 1300 K in jet stirred or plug flow reactors [14, 26] and up to 1750 K in shock tubes [5, 27]. Within the range of conditions reported, formation of alkyl radicals is commonly observed and the dominance of several radicals depending on the temperature are discussed [26, 28, 29]. In our simulations, decomposition of n-dodecane is observed to be involving a variety of reactions, including H abstraction (R1,R2), alkyl abstraction (R3-R7), and homolytic cleavage (R8), each contributing to the complex mechanisms of soot formation. Reactions having more than three products in the simulations' output file are excluded from our analysis, as they are unlikely to occur through a single elementary step. For pure n-dodecane, pathways leading to the larger hydrocarbons through ethyl, methyl and butyl abstraction (R4-R6) dominate with contributions of 20.0%, 16.5% and 19.0%, respectively. Addition of m-xylene shifts the decomposition towards the higher contributions from H abstraction (R1,R2) and the pathways involving smaller hydrocarbons. In the presence of oxygen, the influence of oxidative conditions reduces the contributions of large fragments such as $C_{10}H_{21}$, while increasing the role of pathways producing species like C_8H_{17} and smaller hydrocarbons. These patterns imply that the reaction network is considerably changed by the presence of oxygen and m-xylene, promoting hydrogen abstraction and fragmentation. However, the effect of oxygen on the global decay rate of n-dodecane is observed to be inconsequential since oxidative pathways are not dominated at high temperatures. The above also highlight evidence of cross-chemical interactions, which are typically not addressed in chemical mechanisms [30].

Table 2 Initial decomposition reactions of n-dodecane at 2500 K.

R#	Reactions	<i>n</i> -dodecane	<i>n</i> -dodecane + <i>m</i> -xylene	<i>n</i> -dodecane + <i>m</i> -xylene + O ₂
R1	$C_{12}H_{26} \rightarrow C_{12}H_{25} + H$	6.0%	9.5%	10.0%
R2	$C_{12}H_{26} + H \rightarrow C_{12}H_{25} + H_2$			
R3	$C_{12}H_{26} \rightarrow C_{11}H_{23} + CH_3$	4.5%	3.0%	4.5%
R4	$C_{12}H_{26} \rightarrow C_{10}H_{21} + C_2H_5$	20.0%	11.0%	13.5%
R5	$C_{12}H_{26} \rightarrow C_9H_{19} + C_3H_7$	16.5%	23.5%	16.0%
R6	$C_{12}H_{26} \rightarrow C_8H_{17} + C_4H_9$	19.0%	20.0%	19.0%
R7	$C_{12}H_{26} \rightarrow C_7H_{15} + C_5H_{11}$	15.5%	15.5%	21.5%
R8	$C_{12}H_{26} \rightarrow C_6H_{13} + C_6H_{13}$	10.5%	6.5%	7.5%

In Fig. 4, formation of C2, C3 and C4 species are reported at 2500 K. C2-C4 hydrocarbons are predominantly produced from the initial decomposition reactions of n-dodecane within 0.2 ns, as well as from the further interactions of formed radicals with the other species. These small hydrocarbons have a key role on the formation of aromatics via being consumed to form larger carbon clusters. While the rate of formation of C2 hydrocarbons are comparably similar with the addition of *m*-xylene and oxygen, the presence of aromatics enhances the formation of C3 hydrocarbons at early stages and C4 hydrocarbons after the complete decay of n-dodecane molecules.

**Fig. 4 Time dependent (a) C2 (b) C3 and (c) C4 species formation at 2500 K.**

Further analysis on the chemical pathway from the decomposition of hydrocarbons to the growth of carbon clusters reveals that the aromatic compounds are formed from small hydrocarbons and radicals, leading to the larger Polycyclic Aromatic Hydrocarbons (PAHs) and eventually soot clusters. Fig. 5 demonstrates the breakdown of n-dodecane and subsequent the chemical reactions that produce smaller hydrocarbons and the first aromatic ring, phenyl radical (C_6H_5). The cleavage of C-C or C-H bonds initiates the breakdown of n-dodecane into phenyl, producing alkyl radicals, i.e. C_8H_{17} and C_4H_9 . Smaller hydrocarbons such as propene (C_3H_6) and ethylene (C_2H_4) are formed when these radicals go through a sequence of C-C cleavage and hydrogen abstraction reactions. The resultant intermediates, such as C_5H_7 and C_9H_{11} , help to form bigger unsaturated molecules that go through cyclization as the reaction proceeds. Phenyl radicals are the final products of further stabilizing these cyclic intermediates by hydrogen abstraction or methyl loss. It will eventually form more stable and complex PAHs leading to the formation of soot clusters.

Fig. 6 shows that the addition of m-xylene to n-dodecane significantly alters the pathway to phenyl formation. The decomposition of m-xylene starts with the abstraction of a methyl group, producing toluene radical, C_7H_7 . In the meantime, n-dodecane decomposes into larger hydrocarbons (C_6H_{13} and C_3H_6) compared to the pure n-dodecane case, and the products react with toluene radical to form more stable form, toluene (C_7H_8). After removal of the methyl group, a phenyl radical forms from toluene. The aromatic ring of m-xylene accelerates the production of aromatic compounds without needing smaller hydrocarbons produced from the pyrolysis of n-dodecane, as it requires fewer reaction steps.

The pathways for n-dodecane and n-dodecane + m-xylene to phenyl differ significantly in complexity. Since the n-dodecane pathway heavily fragments into smaller aliphatic hydrocarbons and then forms aromatic rings through cyclization, the process of aromatic synthesis becomes more complicated and takes longer. The aromatic structure of m-xylene, on the other hand, offers an accelerated route to phenyl by requiring fewer reaction steps and chemical intermediates. C_3H_5 plays an important role in both pathways for the formation of the phenyl radical. As indicated in Table 2, methyl abstraction is the most probable reaction in the presence of m-xylene making the aromatics formation more favorable. It is also observed that introducing oxygen does not have an impact on the chemical pathway to the formation of first aromatic ring in the presence of m-xylene since the kinetics are mostly driven by the thermal decomposition of fuel molecules at high temperature conditions. It slightly enhances the rate of n-dodecane decomposition by altering the initial decomposition steps, as it is reported in Table 2.

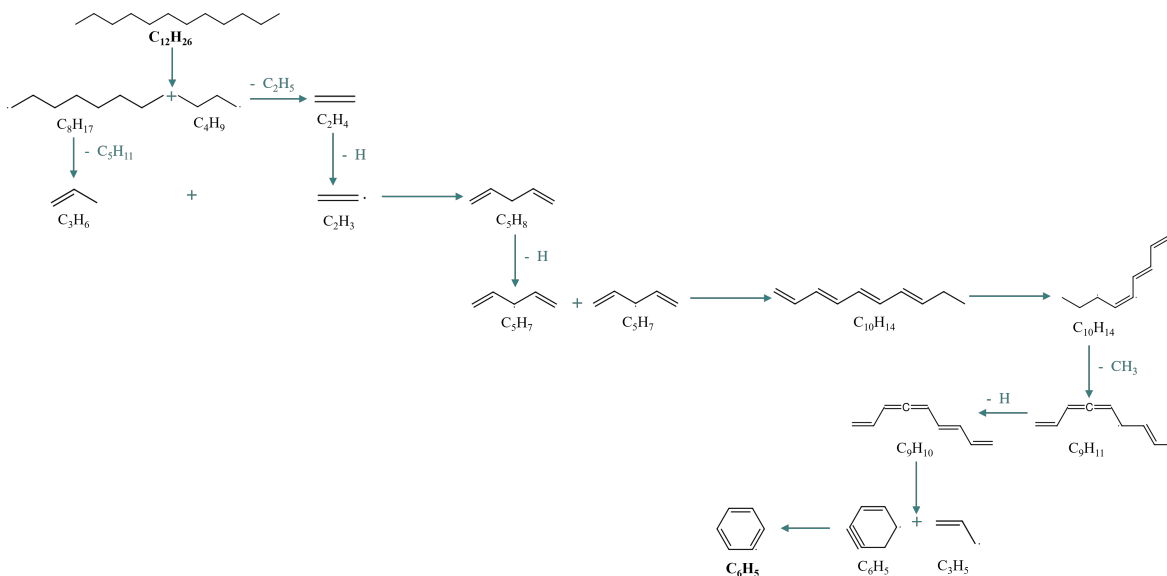


Fig. 5 Reaction pathway to the formation of phenyl radical from n-dodecane at 2500 K.

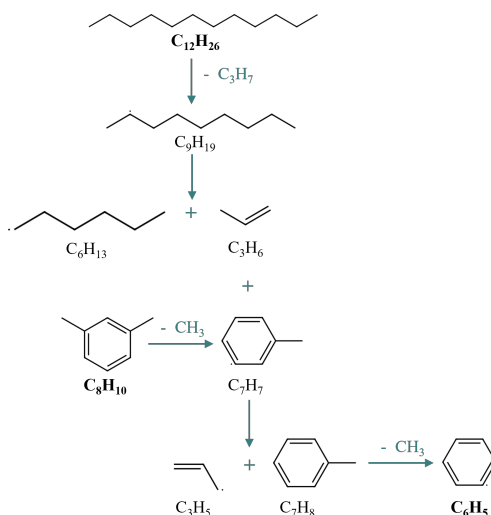
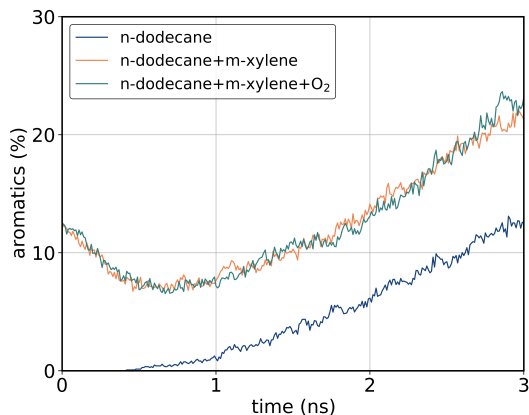


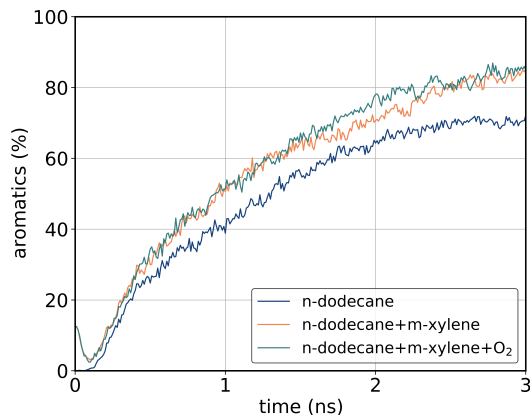
Fig. 6 Reaction pathway to the formation of phenyl radical from n-dodecane + m-xylene at 2500 K.

Aromatic compounds serve as key intermediates in soot formation, contributing to the growth and aggregation of soot particles due to their inherent stability and resonance characteristics [31]. Therefore, the formation rate of aromatics are analyzed at the performed conditions and reported in Fig. 7. Since the low temperature simulations capture the chemistry in realistic engine conditions, it will be more accurate to analyze the effect of m-xylene and oxygen on the aromatics formation at these conditions. As indicated in Fig. 7a, the formation of aromatics from pure n-dodecane starts more slowly since several elementary reactions need to happen to form the first aromatic ring and at the end of 3 ns, only the 13% of the compounds have aromatic features at 2500 K. The addition of m-xylene significantly increases the aromatic content formed during the process, rising to 26% with and without oxygen. As it is analyzed in the phenyl formation mechanism reported in Fig. 6, m-xylene molecules need to break down to aromatic radicals in order to grow more stable PAH structures. This trend can be observed in Fig. 7a up to 0.8 ns. While the initial rate of formation of aromatics are very similar with and without m-xylene, it certainly accelerates as less aliphatics present inside the domain, i.e. after 2.2 ns. These trends highlight that the growth of larger PAHs in a shorter duration is expected in the presence of aromatic hydrocarbons. The effect of 3% O_2 on the aromatics formation cannot be observed under the performed conditions. Further analysis will be performed by altering the composition of O_2 .

It should also be mentioned that the final most carbonaceous product of low temperature simulations after 3 ns are $C_{19}H_{15}$, $C_{22}H_{14}$ and $C_{27}H_{17}$ for n-dodecane, n-dodecane + m-xylene and n-dodecane + m-xylene + O_2 , respectively. Since it will take more time to produce large soot clusters at 2500 K, high temperature simulations are performed at 3500 K and its aromatics formation rate is reported in Fig. 7b. In order to ensure that the chemistry is acceptably captured at high temperature simulations, the slope of the aromatic formation curves up to 12% aromatics are compared. At 2500 K, the slope of the aromatic formation curve is calculated as 4.55 %/ns, whereas at 3500 K, it is 46.3 %/ns. This indicates that the simulations at the higher temperature are accelerated approximately 10 times compared to those at 2500 K. The acceleration factor carries an error margin of 1.76%, confirming that the observed impact of elevated temperatures on the formation of aromatic species and carbon clusters is relatively minor in MD perspective. Formation of ethylene, being one of the major products of dodecane pyrolysis, is also given in Fig. 8 for 2500 K and 3500 K simulations for comparison. While the amount of ethylene molecule formed is nearly the same, the consumption rate of ethylene is significantly increased with the increase in temperature. This acceleration with temperature allows us to perform nanoscale simulations to create carbon/soot clusters within a reasonable computational time. Therefore, larger soot particles are created at 3500 K and their structural properties are compared in order to understand the effect of aromatics and oxygen on the soot morphology.

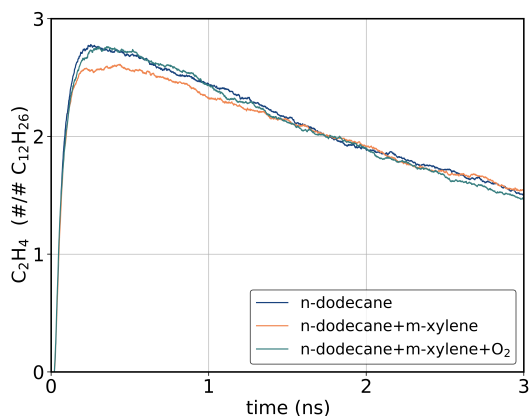


(a)

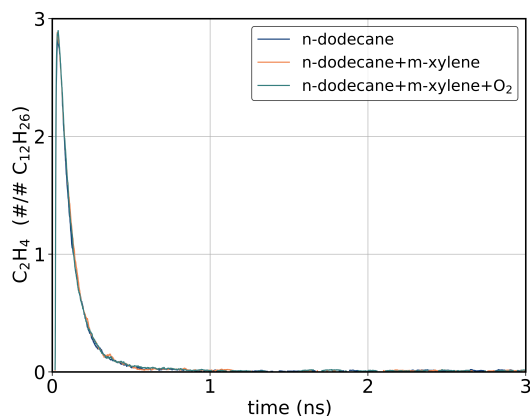


(b)

Fig. 7 Time dependent aromatic species formation at (a) 2500 K and (b) 3500 K.



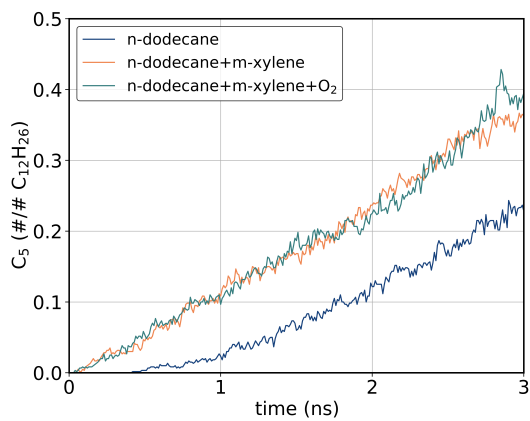
(a)



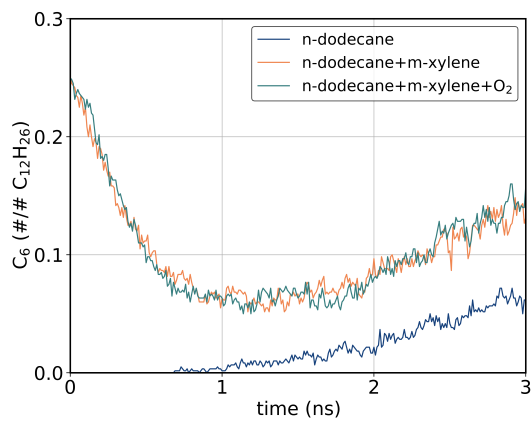
(b)

Fig. 8 Time dependent ethylene (C_2H_4) formation at (a) 2500 K and (b) 3500 K.

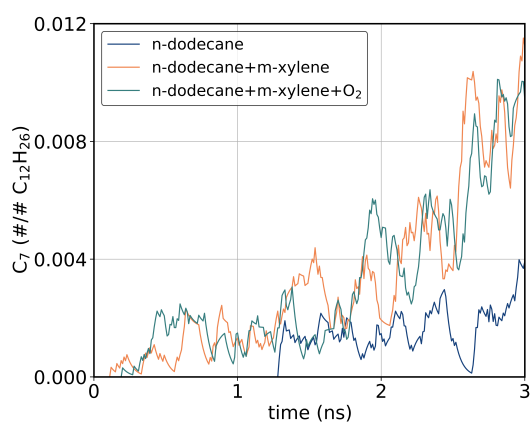
Formation of 5-membered (C5), 6-membered (C6) and 7-membered (C7) rings has a crucial importance on the morphology of the soot particle [32]. It has been observed that the presence of 5- and 7-membered rings on aromatic structures causes curvature on the soot structure resulting in less graphitic stacks, smaller particle size and higher oxidation rates [32, 33]. Hence, the formation of C5, C6 and C7 cyclic hydrocarbons at 2500 K and 3500 K are reported in Fig. 9 and Fig. 10, respectively. Low temperature simulations captures the formation of ring structures well at the initial stages of pyrolysis. While the aliphatic C5-C7 hydrocarbons are formed within 0.2 ns from the thermal decomposition of n-dodecane as reported in Table 2, ring structured hydrocarbons started to form after the maximum production of C2-C3 hydrocarbons. Hydrocarbons with 6-membered rings formation has a very similar trend with the aromatics formation. At higher temperatures, the total amount of 6-membered hydrocarbons and their rate of formations are quite comparable for all cases, the formation of odd-numbered hydrocarbons shows the highest yield in the presence of m-xylene, with and without oxygen. Since the majority of the structures are 6-membered, the morphological properties of the formed soot particles are expected to be similar. Hence, the presence of m-xylene significantly increases the reaction rates and final concentrations of all higher membered rings, indicating their synergistic effect in rapidly breaking down n-dodecane and producing soot precursors.



(a)

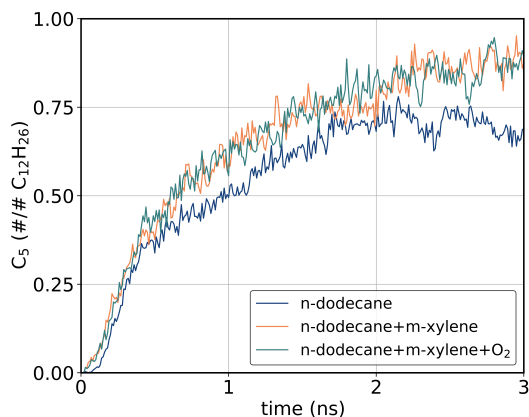


(b)

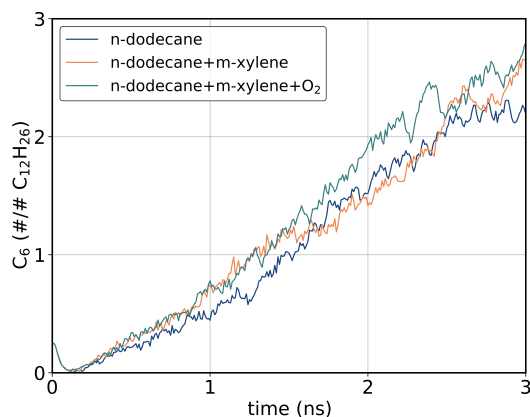


(c)

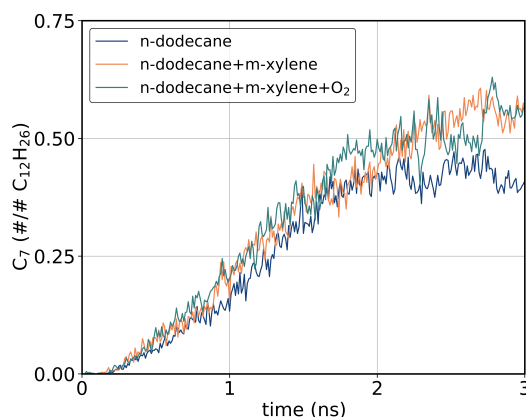
Fig. 9 Time dependent (a) 5- (b) 6- and (c) 7-membered rings formation at 2500 K.



(a)



(b)



(c)

Fig. 10 Time dependent (a) 5- (b) 6- and (c) 7-membered rings formation at 3500 K.

The formation and the nucleation of large hydrocarbon clusters over time at 3500 K is reported in Fig. 11. The same mechanism of the soot formation including nucleation, growth and agglomeration is observed for all molecular configurations studied. Hence, the snapshots are reported only for n-dodecane molecules as a representation. At 0.5 ns as given in Fig. 11a, scattered small hydrocarbons, mainly the products of pyrolysis reactions, are observed in addition to the species with isolated aromatic rings. By 1.0 ns, the onset of the nucleation can clearly be observed. Clusters are grown into larger structures as PAHs begin to agglomerate. Most of the larger hydrocarbon contains both aromatic rings and long aliphatic chains transitioning into soot precursors. At 1.5 ns, a graphitic dense hydrocarbon cluster emerges from the growth of PAHs. Surface growth still continues with the addition of aromatic species formed inside the domain as the nascent particle is evolving to a fullerene-like structure.

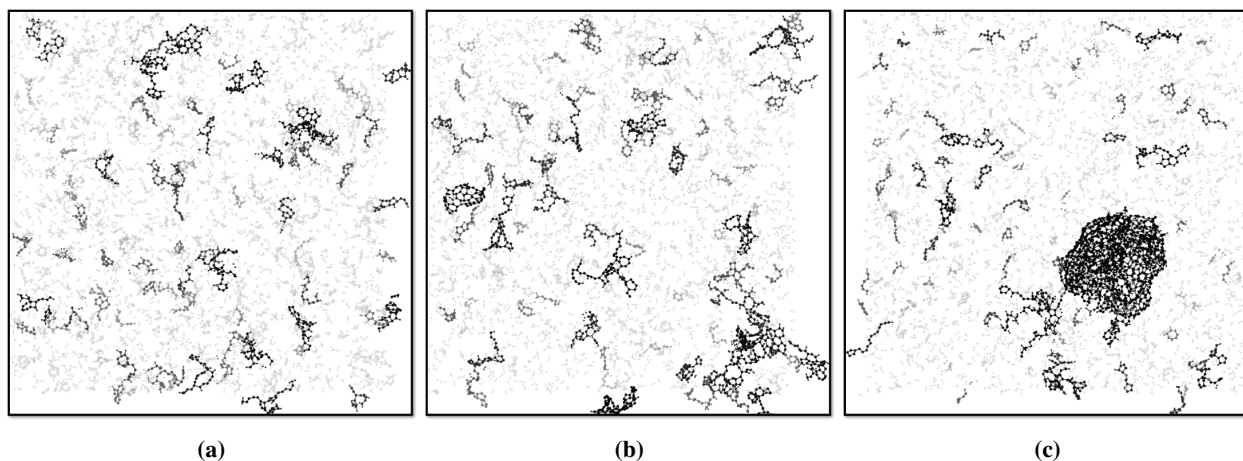


Fig. 11 Formation of hydrocarbon clusters from n-dodecane molecules at 3500 K (a) 0.5 ns (b) 1.0 ns and (c) 1.5 ns. Larger clusters are highlighted in gray and black.

Fig. 12 reports the temporal evolution of the mass of the most carbonaceous hydrocarbon at 3500 K. The slowest rate of soot generation is observed for pure n-dodecane, where it increases steadily and gradually over time due to the formation of radicals and the interactions between them to form aromatic clusters and aggregates. The steeper slope in the soot mass curve indicates that adding m-xylene to n-dodecane greatly enhances soot mass production. In the presence of oxygen, the soot formation rate is the highest, reaching the largest soot mass within 3 ns. Since the effect of oxygen is not observed at the initial stages of pyrolysis and aromatics formation, it is expected that the radicals forming from oxygen, i.e. OH, have a significant impact on the later stages of surface growth by possibly reacting with aromatic radicals and stabilizing them into coagulated structures.

The fluctuations at the later stages of the simulation (after 2.5 ns) could indicate the stability of the particle and the restructuring of the carbon cluster. As it is observed from Fig. 12, the most stable soot structure is formed in the presence of m-xylene and O₂ together as it shows minimal fluctuations at the later stages. While m-xylene yields the formation of aromatic radicals, oxygenated radicals can stabilize the formed clusters. It should be emphasized that the different chemical structures and oxidative environment have a crucial impact on every stage of the soot formation, as well as on the morphological properties of the formed carbon clusters.

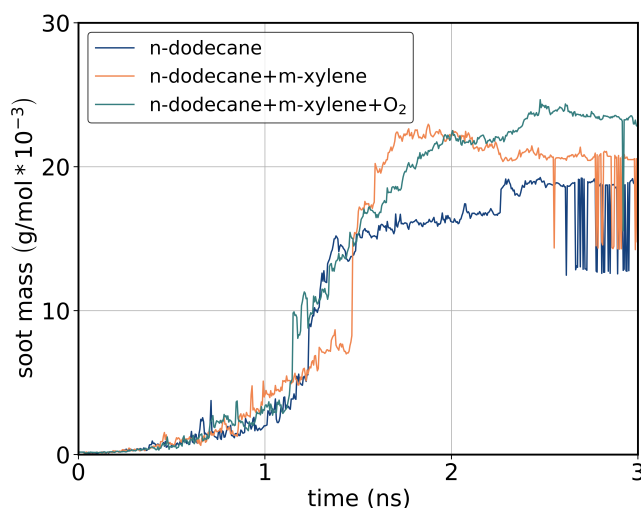
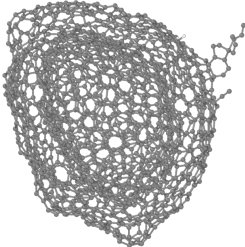
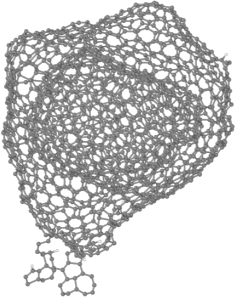
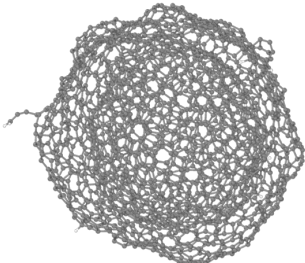


Fig. 12 Change in the mass of the largest carbon cluster at 3500 K.

In Table 3, soot clusters formed at 3500 K after 3 ns are reported. More than 60% of the carbon atoms in the domain

are coagulated and created one large carbon cluster at a simulated time of 3 ns. All of the particles have very large C/H ratios indicating that the formed particles are highly mature and stable. However, the oxygenated case has the lowest value, possibly due to the interaction of surface atoms with oxygenated radicals. While the sizes of the particles are comparable, the particle originating from pure n-dodecane is comparably smaller, the largest being the particle formed from n-dodecane, m-xylene and oxygen. While the result of the largest particle coming from the simulation case with oxygen is inconsistent with experimental results by Sim et al. [34], the temperature conditions are drastically different. Sim and coworkers observed significant oxidation of soot at temperatures up to 1700 K, in environments containing small amounts of oxygen (from 1 to 5 %). The present results support the small effect of oxidation at such elevated temperatures, which is in agreement with the observations regarding the molecular decomposition of the hydrocarbons shown in Fig. 2 and 3. The formation of odd-membered rings also supports the size change between the simulated cases. There is no significant difference in the aromatic contents of the soot particles. It can be interpreted that even without the presence of aromatics at the initial configuration of molecules, comparably similar soot particles can form from long aliphatic hydrocarbons through pyrolytic and cyclization reactions. Each particle has graphene-like structures at the beginning of growth process, while they eventually become more like fullerene type of incipient and mature particles with high aromatic content. The addition of m-xylene and oxygen could influence the formation of larger and more condensed aromatic rings, resulting in higher carbon values even with similar aromatics percentages.

Table 3 Properties of the soot particles formed at 3500 K at a simulated time of 3 ns.

	<i>n-dodecane</i>	<i>n-dodecane + m-xylene</i>	<i>n-dodecane + m-xylene + O₂</i>
			
C_{\max}	1572	1756	1901
$(C/H)_{\max}$	157.2	159.6	126.7
rg (nm)	1.34	1.44	1.47
% aromatics	98.86	97.76	98.84

V. Conclusion

This study investigated the formation of soot from n-dodecane and its blend with m-xylene under pyrolytic and low-oxygen conditions using reactive MD simulations. The pyrolysis rate of n-dodecane at 2500 K observed to be only slightly affected by the addition of m-xylene and oxygen, although these components introduced a complexity to the reaction network introducing more pathways and intermediates. Phenyl radical formation is observed from n-dodecane pyrolysis to possibly serve as a nuclei for further growth to larger carbon clusters. For the studied systems, aromatic compounds are observed to be insufficient to directly initiate soot formation but result in the formation of more aromatic hydrocarbons and PAHs. The driving mechanism for phenyl formation in the presence of m-xylene passes through the toluene radical formation with less elementary steps than pure n-dodecane. There are no major changes in the chemical pathway towards the phenyl formation observed in the presence of 3 % oxygen.

High temperature simulations at 3500 K are performed in order to form larger carbon clusters within the same time frame. Soot particles with radii of 1-1.5 nm evolved from graphene-like to fullerene-like structures with high aromatic content. The addition of m-xylene and oxygen resulted in slightly larger soot particles with higher carbon content, promoting the growth and agglomeration of soot particles. The initial results of this study provide valuable insights into soot formation under engine-relevant conditions, highlighting the importance of initial fuel composition and oxygen presence in determining soot particle size and structure. These findings contribute to a deeper understanding of soot and

contrail formation mechanisms, crucial for developing strategies to mitigate soot emissions and their environmental impact in aviation. Further research focusing on detailed chemical pathway analysis will provide additional clarity on the role of various intermediates and radicals in soot formation.

Acknowledgments

Sandia National Laboratories is a multi-mission laboratory managed and operated by National Technology & Engineering Solutions of Sandia, LLC (NTESS), a wholly owned subsidiary of Honeywell International Inc., for the U.S. Department of Energy's National Nuclear Security Administration (DOE/NNSA) under contract DE-NA0003525. This written work is authored by an employee of NTESS. The employee, not NTESS, owns the right, title and interest in and to the written work and is responsible for its contents. Any subjective views or opinions that might be expressed in the written work do not necessarily represent the views of the U.S. Government. The publisher acknowledges that the U.S. Government retains a non-exclusive, paid-up, irrevocable, world-wide license to publish or reproduce the published form of this written work or allow others to do so, for U.S. Government purposes. The DOE will provide public access to results of federally sponsored research in accordance with the DOE Public Access Plan. FJG was supported by the Transformational Tools and Technologies Project under the NASA Aeronautics Research Mission Directorate.

References

- [1] Lee, D. S., Fahey, D. W., Skowron, A., Allen, M. R., Burkhardt, U., Chen, Q., Doherty, S. J., Freeman, S., Forster, P. M., Fuglestad, J., et al., "The contribution of global aviation to anthropogenic climate forcing for 2000 to 2018," *Atmospheric environment*, Vol. 244, 2021, p. 117834.
- [2] Kärcher, B., "Formation and radiative forcing of contrail cirrus," *Nature communications*, Vol. 9, No. 1, 2018, p. 1824.
- [3] Lee, D. S., Allen, M. R., Cumpsty, N., Owen, B., Shine, K. P., and Skowron, A., "Uncertainties in mitigating aviation non-CO₂ emissions for climate and air quality using hydrocarbon fuels," *Environmental Science: Atmospheres*, Vol. 3, No. 12, 2023, pp. 1693–1740.
- [4] Riebl, S., Braun-Unkhoff, M., and Riedel, U., "A study on the emissions of alternative aviation fuels," *Journal of Engineering for Gas Turbines and Power*, Vol. 139, No. 8, 2017, p. 081503.
- [5] Malewicki, T., and Brezinsky, K., "Experimental and modeling study on the pyrolysis and oxidation of n-decane and n-dodecane," *Proceedings of the combustion institute*, Vol. 34, No. 1, 2013, pp. 361–368.
- [6] Karataş, A. E., and Gülder, Ö. L., "Soot formation in high pressure laminar diffusion flames," *Progress in Energy and Combustion Science*, Vol. 38, No. 6, 2012, pp. 818–845.
- [7] Böhm, H., Jander, H., and Tanke, D., "PAH growth and soot formation in the pyrolysis of acetylene and benzene at high temperatures and pressures: Modeling and experiment," *Symposium (international) on combustion*, Vol. 27, Elsevier, 1998, pp. 1605–1612.
- [8] Zador, J., Fellows, M. D., and Miller, J. A., "Initiation reactions in acetylene pyrolysis," *The Journal of Physical Chemistry A*, Vol. 121, No. 22, 2017, p. 4203–4217.
- [9] Krestinin, A., "Detailed modeling of soot formation in hydrocarbon pyrolysis," *Combustion and Flame*, Vol. 121, No. 3, 2000, pp. 513–524.
- [10] Skeen, S. A., and Yasutomi, K., "Measuring the soot onset temperature in high-pressure n-dodecane spray pyrolysis," *Combustion and Flame*, Vol. 188, 2018, pp. 483–487.
- [11] Zeng, M., Yuan, W., Li, W., Zhang, Y., and Wang, Y., "Investigation of n-dodecane pyrolysis at various pressures and the development of a comprehensive combustion model," *Energy*, Vol. 155, 2018, pp. 152–161.
- [12] Kashiwa, K., Arai, M., and Kobayashi, Y., "Oxygen effect on PAH and PM formation in low temperature benzene pyrolysis," *Fuel*, Vol. 262, 2020, p. 116429.
- [13] Busillo, E., Vlasov, P., and Arutyunov, V., "Influence of oxygen on soot formation during acetylene pyrolysis," *Mendeleev Communications*, Vol. 32, No. 5, 2022, pp. 700–702.
- [14] Herbinet, O., Marquaire, P.-M., Battin-Leclerc, F., and Fournet, R., "Thermal decomposition of n-dodecane: Experiments and kinetic modeling," *Journal of Analytical and Applied Pyrolysis*, Vol. 78, No. 2, 2007, pp. 419–429.

- [15] Friesner, R. A., “Ab initio quantum chemistry: Methodology and applications,” *Proceedings of the National Academy of Sciences*, Vol. 102, No. 19, 2005, pp. 6648–6653.
- [16] Van Duin, A. C., Dasgupta, S., Lorant, F., and Goddard, W. A., “ReaxFF: A reactive force field for hydrocarbons,” *The Journal of Physical Chemistry A*, Vol. 105, No. 41, 2001, pp. 9396–9409.
- [17] Liang, T., Shin, Y. K., Cheng, Y.-T., Yilmaz, D. E., Vishnu, K. G., Veners, O., Zou, C., Phillpot, S. R., Sinnott, S. B., and Van Duin, A. C., “Reactive potentials for advanced atomistic simulations,” *Annual review of materials research*, Vol. 43, No. 1, 2013, pp. 109–129.
- [18] Zhang, C., Zhang, C., Ma, Y., and Xue, X., “Imaging the C black formation by acetylene pyrolysis with molecular reactive force field simulations,” *Physical Chemistry Chemical Physics*, Vol. 17, No. 17, 2015, pp. 11469–11480.
- [19] Wang, Q.-D., Wang, J.-B., Li, J.-Q., Tan, N.-X., and Li, X.-Y., “Reactive molecular dynamics simulation and chemical kinetic modeling of pyrolysis and combustion of n-dodecane,” *Combustion and Flame*, Vol. 158, No. 2, 2011, pp. 217–226.
- [20] Martínez, L., Andrade, R., Birgin, E. G., and Martínez, J. M., “PACKMOL: A package for building initial configurations for molecular dynamics simulations,” *Journal of computational chemistry*, Vol. 30, No. 13, 2009, pp. 2157–2164.
- [21] Plimpton, S., “Fast parallel algorithms for short-range molecular dynamics,” *Journal of computational physics*, Vol. 117, No. 1, 1995, pp. 1–19.
- [22] Thompson, A. P., Aktulga, H. M., Berger, R., Bolintineanu, D. S., Brown, W. M., Crozier, P. S., In’t Veld, P. J., Kohlmeyer, A., Moore, S. G., Nguyen, T. D., et al., “LAMMPS—a flexible simulation tool for particle-based materials modeling at the atomic, meso, and continuum scales,” *Computer Physics Communications*, Vol. 271, 2022, p. 108171.
- [23] Ashraf, C., and Van Duin, A. C., “Extension of the ReaxFF combustion force field toward syngas combustion and initial oxidation kinetics,” *The Journal of Physical Chemistry A*, Vol. 121, No. 5, 2017, pp. 1051–1068.
- [24] Döntgen, M., Przybylski-Freund, M.-D., Kröger, L. C., Kopp, W. A., Ismail, A. E., and Leonhard, K., “Automated discovery of reaction pathways, rate constants, and transition states using reactive molecular dynamics simulations,” *Journal of chemical theory and computation*, Vol. 11, No. 6, 2015, pp. 2517–2524.
- [25] Mukut, K. M., Roy, S., and Goudeli, E., “Molecular arrangement and fringe identification and analysis from molecular dynamics (MAFIA-MD): A tool for analyzing the molecular structures formed during reactive molecular dynamics simulation of hydrocarbons,” *Computer Physics Communications*, Vol. 276, 2022, p. 108325.
- [26] Dahm, K., Virk, P., Bounaceur, R., Battin-Leclerc, F., Marquaire, P., Fournet, R., Daniau, E., and Bouchez, M., “Experimental and modelling investigation of the thermal decomposition of n-dodecane,” *Journal of Analytical and Applied Pyrolysis*, Vol. 71, No. 2, 2004, pp. 865–881.
- [27] MacDonald, M. E., Ren, W., and Yangye, “Fuel and ethylene Measurements during n-dodecane, methylcyclohexane, and iso-cetane pyrolysis in shock tubes,” *Fuel*, Vol. 103, 2013, pp. 1060–1068.
- [28] Banerjee, S., Tangko, R., Sheen, D. A., Wang, H., and Bowman, C. T., “An experimental and kinetic modeling study of n-dodecane pyrolysis and oxidation,” *Combustion and Flame*, Vol. 163, 2016, pp. 12–30.
- [29] Yikai, L., Zhang, J., Yujun, L., Zhang, D., Cui, N., Kun, W., Zhang, T., and Fan, X., “Experimental and kinetic study of high pressure pyrolysis of n-dodecane,” *Journal of Analytical and Applied Pyrolysis*, Vol. 170, 2023, p. 105908.
- [30] Vermeire, F. H., Aravindakshan, S. U., Jocher, A., Liu, M., Chu, T.-C., Hawtof, R. E., Van de Vijver, R., Prendergast, M. B., Van Geem, K. M., and Green, W. H., “Detailed kinetic modeling for the pyrolysis of a jet a surrogate,” *Energy & Fuels*, Vol. 36, No. 3, 2022, pp. 1304–1315.
- [31] Gleason, K., Carbone, F., Sumner, A. J., Drollette, B. D., Plata, D. L., and Gomez, A., “Small aromatic hydrocarbons control the onset of soot nucleation,” *Combustion and Flame*, Vol. 223, 2021, pp. 398–406.
- [32] Abdrabou, M. K., Morajkar, P. P., Peña, G. D. G., Raj, A., Elkadi, M., and Salkar, A. V., “Effect of 5-membered bicyclic hydrocarbon additives on nanostructural disorder and oxidative reactivity of diffusion flame-generated diesel soot,” *Fuel*, Vol. 275, 2020, p. 117918.
- [33] Vander Wal, R. L., and Tomasek, A. J., “Soot oxidation: dependence upon initial nanostructure,” *Combustion and flame*, Vol. 134, No. 1-2, 2003, pp. 1–9.
- [34] Sim, H. S. S., Cenker, E., Choi, E. C., Wan, K. W., Skeen, S. A. S., and Manin, J., “Experimental and numerical study of soot formation in hydrocarbon sprays under high-pressure fuel pyrolysis conditions,” *Applications in Energy and Combustion Science*, 2024, Accepted for publication.